J Mater Sci (2008) 43:3180–3188
DOI 10.1007/s10853-008-2452-1

Cold forging of sintered hollow polygonal disks with barreling

P. Das · Goutam Sutradhar · T. Chakraborty · S. Patra · M. Mitra

Received: 12 April 2007 / Accepted: 7 January 2008 / Published online: 11 March 2008

Abstract The forging of sintered metal-powder performs creates a lot of interest throughout the world as one of the most economic method of manufacturing techniques. This process becomes more popular due to its simplicity and flexibility. During compression of regular polygonal disk between a pair of flat dies both bulging and barreling occurs simultaneously. Theoretical analysis considering bulging and barreling together is highly complicated and in this article an upper bound solution has been constructed for determining the die pressures developed during the compression of hollow polygonal disks taken into account the barreling only. The results so obtained are discussed critically to illustrate the interacted of various process parameters involved and presented graphically.

Nomenclatures

A	Perpendicular distance from center of disk to its outer edge
B	Perpendicular distance from center of disk to its inner edge
$2b$	Length of the side of polygon
h	Half thickness of the specimen
k	Constant(equal to 2)
p_{av}	Average pressure at the die/work piece interface
S	Surface of velocity discontinuity
$\|\Delta V\|$	Magnitude of velocity discontinuity
η	Constant; a function only
ρ	Initial relative density of the preform
σ	Yield stress of the non-work hardening matrix metal
σ_0'	Yield stress of the porous material
τ	Shear stress

Introduction

During forging of a hollow polygonal disk between a pair of flat dies, the material flow developed is non-uniform both in the plane section of the disk and along its thickness. We shall call the non-uniformity of flow in the plane section as *bulging* and that along the thickness of the disk as *barreling*. Both these effects are invariably present during forging of any non-circular disk, but to varying degrees depending upon the conditions of forging operation, which, for a regular hollow polygonal disk are:

- The frictional stress at the interface between the dies and the disk,
- Value of the ratio "R" (perpendicular distance from center of the polygonal disk to its edge) for the hollow polygonal disk,

P. Das
W.B. Technical Education, Bikash Bhawan, Salt Lake, Kolkata 700 064, India

G. Sutradhar (✉)
Department of Mechanical Engineering, Jadavpur University, Kolkata 700 032, India
e-mail: goutam_sutradhar@rediffmail.com

T. Chakraborty
Kalyani Government Engineering College, Kalyani, W.B., India

S. Patra
Central Workshop & Instruments Section, Indian Institute of Technology, Kharagpur 721 302, India

M. Mitra
Dean of Faculty of Engineering, Jadavpur University, Kolkata 700 032, India

- The number of sides "N" of the polygonal disk.

It has been established that in case of wrought materials, with low value of R and high value of N, barreling is significant while bulging is negligible. Similarly, with high value of R and low value of N, the bulging is predominant and along with low friction the barreling may be insignificant [1]. However an attempt has been made to verify the above observation in case of sintered samples. Analytical treatment of both barreling and bulging taken together is highly complicated and the solutions of the equations of polygonal disks under deformation were obtained earlier considering only barreling effect [2]. It is reported by earlier research [5–7] regarding the deformation characteristics of sintered polygonal discs but no work has been reported so far on the hollow polygonal discs. In this study an upper bound solution is made for open die forging of regular polygonal disks taking into account the barreling effect only and during the analysis an appropriate interfacial law for porous metals has been used which is of composite nature, which is due to adhesion and sliding. It is expected that the present study will be of great importance for the assessment of die load during the hollow regular metal-powder polygonal disks.

Interfacial friction

The frictional conditions between the tool and the work piece in metal working are of greatest importance concerning a number of factors, such as force and mode of deformation, the properties of finished specimen and the resulting surface finish. The relative velocity between the work piece material and the surface of the forging die, together with high interfacial pressure and/or deformation modes, creates the conditions promoting adhesion in addition to sliding.

In an investigation of the plastic deformation of metal-powder preforms, it is evident that with the application of compressive hydrostatic stress the pores will close and the relative density will increase, whereas with the application of tensile hydrostatic stress the pores will grow and the relative density will decrease. The density distribution also does not seem to be uniform throughout, being high in the central region and low at the edges. The density distribution will be more uniform with smaller coefficient of friction μ and for a greater initial density.

During the forming of metal-powder preforms the compressive force gradually increases the relative density, which is latter directly proportional to the real area of contact. The relative density gradually approaches the apparent relative density, this approach probably being asymptotic.

During the sinter-forging process it is very important to keep special consideration on the interfacial friction, as this will determine the success or failure of the operation. The relative velocity between the work piece material and the die surface, together with high interfacial pressure and or deformation modes, creates a condition of composite friction, which is due to adhesion and sliding. The shear equation becomes $\tau = \mu(p + \rho_0\varphi_0)$, the first term μp being due to sliding and the second term $\mu\rho_0\varphi_0$, being due to adhesion, which latter arises from change of the relative density of the preform during the process. Keeping all these factors in mind the appropriate expression for shear stress in this particular case would be something of the form [3],

$$\tau = \mu[p + \rho_0\varphi_0\{1 - r_m/(b\sec\pi/N)\}1/n], \quad (1)$$

where, r_m = radius of sticking zone for axi-symmetric condition, b = half the length of the side of the polygon, n = constant quantity (and $\gg 1$), N = number of sides of the polygonal disk.

Load bounding technique

Wittenaur [4] has extensively applied methods, which are simpler than the slip line field technique and can be applied to a range of metal working problems to obtain estimates of working loads. Their procedure is to determine a lower limit, or bound, which is certainly too low a load to deform the metal, and also to determine an upper bound, which is certainly too high. The real load must be then between these limits, and the skill in application of the method lies in choosing deformation patterns which make the difference as small as possible.

The lower bound is found from consideration of stress conditions, paying no attention to internal flow restrictions. It is associated with the principle of maximum work. The distortion caused by application of stress, is such as to cause maximum dissipation of energy. Looked at it in another way, the system tends to reach the state of minimum energy compatible with the equilibrium and yield conditions.

Consequently, any other statically admissible stress system would produce an increment of work at most equal to that produced by the actual system, and probably less. Thus any system derived from stress equilibrium will be either just sufficient or too little to perform the operation. This gives a lower bound; we shall not consider it in detail. Moreover lower bound solutions to problems in metal forming working are not yet well established.

A consideration of upper bounds involves the conditions which have to be fulfilled by the strain increments in a fully plastic body, and does not concern itself with stress equilibrium. In metalworking the upper bound is of great

interest, since it ensures that a particular operation can actually be carried out without exceeding the load predicted. The critical factor here is that plastic volume should not change; that the material is incompressible. The principle of maximum work is used here also, but from the point of view of strain: an element deforms in such a way as to offer maximum resistance. If, therefore, we deduce the stress system from any assumed deformation, which must conform to the kinematics conditions, the value will be greater than, or equal to that actually operating.

Velocity field

The material flow developed during the compression of a regular hollow sintered polygonal disk is not axi-symmetric, but the complete disk may be divided into triangular regions so that identical material flow may be developed. The triangular region OAB with face AA'B'B bounded by the planes A'E'D'B', A'A E E', AEDB, B'BDD', E'EDD', is one such region as shown in Fig. 1. Since the material flow in such region is identical, there is no shear strain or velocity discontinuity along the radial planes connecting the two regions. As already mentioned previously, the barreling effect (that is the non uniformity of flow along the thickness of the disk) is considered in the present analysis.

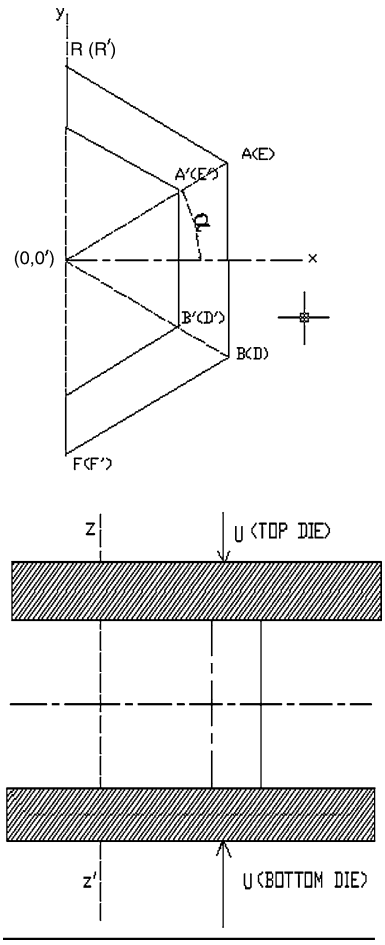

Fig. 1 Velocity field in triangular regions

Now the material flow in the upper half of the trapezoidal region AA'B'B, is the mirror image of that developed in the lower half. Hence, only the upper half of the trapezoidal region AA'B'B of the complete disk is considered for the analysis.

The particle velocities in x and y directions in this region (expressed in Cartesian co-ordinate system) are expressed as

$$U_x = (1+2\eta)/(1-\eta) \times (U/h)xMe^{-\beta z/h}, \tag{2}$$

$$U_y = (1+2\eta)/(1-\eta) \times (U/h)yMe^{-\beta z/h}. \tag{3}$$

The parameter M and β in Eqs. 2 and 3 signify the spread of the facial surfaces of the disk and the extent of barreling, respectively. In fact M is a function of β as determined below. Hence, it is the only unknown parameter in the above equations.

The strain rates in the x and y directions are

$$e_{xx} = (1+2\eta)/(1-\eta) \times (U/h)Me^{-\beta z/h}, \tag{4}$$

$$e_{yy} = (1+2\eta)/(1-\eta) \times (U/h)Me^{-\beta z/h} = e_{xx}. \tag{5}$$

From the condition of compressibility

$$e_{xx} + e_{yy} + e_{zz} = \pm 2\eta\sqrt{[(e_{xx}-e_{yy})^2 + (e_{yy}-e_{zz})^2 + (e_{zz}-e_{xx})^2]} \tag{6}$$

or,

$$e_{zz} = 2(\eta-1)/(1+2\eta)e_{xx} = -2(U/h)Me^{-\beta z/h}. \tag{7}$$

Integrating Eq. 7, one gets

$$U_z = 2UM/\beta e^{-\beta z/h} + f(x,y). \tag{8}$$

Now, at $z = 0$, $U_z = 0$ for all x and y.

And, at $z = h$, $U_z = -U$.

Substituting the above values in Eq. 8, one gets

$$f(x,y) = 2UM/\beta \text{ and } M = \beta/(1-e^{-\beta}).$$

Putting the values of M in above equation, the velocity is determined as

$$U_x = (1+2\eta)/(1-\eta) \times \beta/2(1-e^{-\beta}) \times (U/h)xe^{-\beta z/h}, \tag{9}$$

$$U_y = (1+2\eta)/(1-\eta) \times \beta/2(1-e^{-\beta}) \times (U/h)ye^{-\beta z/h}, \tag{10}$$

$$U_z = U(e^{-\beta z/h}-1)/(1-e^{-\beta}). \tag{11}$$

Corresponding strain rates becomes

$$e_{xx} = \partial U_x/\partial x = (1+2\eta)/(1-\eta) \times \beta/2(1-e^{-\beta}) \times (U/h)e^{-\beta z/h}, \quad (12)$$

$$e_{yy} = \partial U_y/\partial y = (1+2\eta)/(1-\eta) \times \beta/2(1-e^{-\beta}) \times (U/h)e^{-\beta z/h}, \quad (13)$$

$$e_{zz} = -U/(1-e^{-\beta}) \times \beta/h \times e^{-\beta z/h}, \quad (14)$$

$$e_{xy} = e_{yx} = \frac{1}{2}[\partial U_x/\partial y + \partial U_y/\partial x] = 0, \quad (15)$$

$$e_{yz} = e_{zy} = \frac{1}{2}[\partial Uy/\partial z + \partial U_z/\partial y] = -(1+2\eta)/(1-\eta) \times \beta^2 U_y/4h^2(1-e^{-\beta}) \times e^{-\beta z/h}, \quad (16)$$

$$e_{xz} = e_{zx} = -(1+2\eta)/(1-\eta) \times \beta^2 U_x/4h^2(1-e^{-\beta}) \times e^{-\beta z/h}. \quad (17)$$

Upper bound theorem

Conservation of energy for a deforming plastic solid of volume V, surface area S, including inertia body forces may be expressed as [1]

$$J^* = \int F_i U_i \mathrm{d}S = 2/\sqrt{3}\sigma_o' \int \sqrt{(1/2\dot{e}_{ij}\dot{e}_{ij})}\mathrm{d}V + \int_s \tau|\Delta v|\mathrm{d}S + \int_v \rho a_i U_i \mathrm{d}V - \int_{st} \mathbf{T}_i v_i \mathrm{d}S, \quad (18)$$

$$J^* = \int F_i U_i \mathrm{d}S = W_i + W_f + W_a + W_t, \quad (19)$$

where, U_i is the displacement rate field which satisfies the given displacement boundary conditions and the equation of incompressibility. A_i is the associated acceleration field. $\mathbf{T}_i$ stress vector prescribed on surface S_t of zone plastic deformation. $\dot{E}_{ij}$ corresponding strain rate tensor field. ΔV is the relative velocity of the specimen over the surface of the die and is equal to the velocity component of the specimen in the tangential direction at the interface, i.e., magnitude of velocity discontinuity.

In Eq. 18, the first term on the right-hand side denotes the rate of internal energy dissipation W_i, the second term denotes the frictional shear energy, W_f and the third term denotes the energy dissipation due to inertia forces W_a. The last term covers power supplied by pre determined body traction. They are, for example, back stress applied in the process of wire drawing or back and front tension in rolling.

In this particular solution for calculation of forging load for hollow sintered polygonal disk forces due to inertia are negligibly small and no external surfaces traction is stipulated and, therefore, $W_a = W_t = 0$. Now the external power (J^*) supplied by the press through the platens are

$$J^* = \int F_i U_i \mathrm{d}S = W_i + W_f = 2PU$$

Calculation of forging load

$$W_i = 2/\sqrt{3}\sigma_0' \int_v \sqrt{(1/2 e_{ij} e_{ij}\mathrm{d}V)}$$

$$W_i = 2/\sqrt{3}(\rho^k\sigma/1+\eta) \int_v \sqrt{[1/2(e_{xx}^2 + e_{yy}^2 + e_{zz}^2) + e_{xy}^2 + e_{yz}^2 + e_{zx}^2]}\mathrm{d}V$$

where σ_0' is the yield stress of porous material = $2/\sqrt{(\rho^k\sigma/1+\eta)}$

Now, $e_{xy} = 0$,

$$e_{yz} = e_{zy} = -(1+2\eta)/(1-\eta) \times 2/\sqrt{3}(\rho^k\sigma/1+\eta) \times \beta^2 U_y/4h^2(1-e^{-\beta}) \times e^{-\beta z/h},$$

$$e_{zx} = e_{xz} = -(1+2\eta)/(1-\eta) \times \beta^2 U_x/4h^2(1-e^{-\beta}) \times e^{-\beta z/h}.$$

Putting the values of e_{xx}, e_{yy}, e_{zz}, e_{xy}, e_{yz}, e_{zx} in equation above, one gets

$$W_i = 2/\sqrt{3}(\rho^k\sigma/1+\eta) \times U/h \times \beta/(1-e^{-\beta}) \int_v e^{-\beta z/h} \times \sqrt{[1+(1+2\eta)^2/(1-\eta)^2 \times (4h^2+\beta^2 r^2)/8h^2]}\mathrm{d}V.$$

For sake of integration, changing over to cylindrical co-ordinate system, one gets

$$W_i = \sqrt{2}/\sqrt{3}(\rho^k\sigma/1+\eta) \times U/h \times \beta/(1-e^{-\beta}) \int_0^h \int_0^\alpha \int_{B/\cos\theta}^{A/\cos\theta} e^{-\beta z/h} \times \sqrt{[1+(1+2\eta)^2/(1-\eta)^2} \times (4h^2+\beta^2 r^2)/8h^2] r\,\mathrm{d}r\,d\theta\,\mathrm{d}z.$$

The above expression for 'N' number of sides can be simplified to the form of

$$W_i = \sqrt{2}/\sqrt{3}N(\rho^k\sigma/1+\eta) \times U \times \beta/(1-e^{-\beta}) \times 1/h \times [h/\beta \times (1-e^{-\beta})] \int_0^\alpha \int_{B/\cos\theta}^{A/\cos\theta} \sqrt{[1+(1+2\eta)^2} /(1-\eta)^2 \times (4h^2+\beta^2 r^2)/8h^2] r\mathrm{d}r\mathrm{d}\theta.$$

On further simplification we get the expression of W_i as follows:

$$W_i = \sqrt{3}/2\sqrt{2}(N\sigma\rho^k U)/(1+\eta)\times(A^2-B^2)\tan\alpha \times[1+0.25(1+2\eta)^2/(1-\eta)^2+\beta^2(A^2+B^2) \times(1+\tan^2\alpha/3)/32h^2].$$

It is assumed that a frictional stress as expressed in Eq. 1 is acting over the entire contacting surface between the dies and the specimen. Thus W_f can be written as:

$$W_f = 2\int_S \tau\sqrt{(U_x+U_y)}\,dS$$

$$W_f = (1+2\eta)/(1-\eta)\}\times\beta U/(1-e^{-\beta})h \times\int_S e^{-\beta z/h}\,\mu[p+\rho_0\phi_0\{1-r_m/(nb\sec\pi/N)\}]r\,dS.$$

For an N-sided polygon at the plane $z = 0$ (since we are carrying out surface integration) and moving over to cylindrical co-ordinate system for the ease of integration, we get,

$$W_f = \mu\{(1+2\eta)/(1-\eta)\}\times\beta U/(1-e^{-\beta})h \times\int_0^{\alpha}\int_{B/\cos\theta}^{A/\cos\theta}[p+\rho_0\phi_0 \times\{1-r_m/(nb\sec\pi/N)\}]r^2 d\theta\,dr.$$

Since, $\rho_0\phi_0 = mp_{\mathrm{av}}$,

$$W_f = \mu(1+2\eta)/(1-\eta)\}\times\beta U(A^3-B^3) /(1-e^{-\beta})6h[p_{\mathrm{av}}N(A^2-B^2)\tan\alpha\{(\tan\alpha\sec\alpha) +\ln(\sec\alpha+\tan\alpha)\}+mp_{\mathrm{av}}(A^3-B^3)\{(\tan\alpha\sec\alpha) +\ln(\sec\alpha+\tan\alpha)\}-mp_{\mathrm{av}}r_m(nb\sec\pi/N) \times\{(\tan\alpha\sec\alpha)+\ln\sec\alpha+\tan\alpha)\}],$$

where,

$$p_{\mathrm{av}} = p/N(A^2-B^2)\tan\alpha$$

Table 1 Physical and chemical analysis of atomized iron powder

Screen analysis, μm	−150	−106	−75	− 63	−45
	150	+106	+75	+63	+45
Element (wt.%)	C	Si	Mn	S	P
	0.12	0.35	0.15	0.43	0.03

$$W_f = N\mu p_{\mathrm{av}}\{(1+2\eta)/(1-\eta)\}\times\beta U(A^3-B^3) /(1-e^{-\beta})6h\{(\tan\alpha\sec\alpha)+\ln(\sec\alpha+\tan\alpha)\} \times[(A^2-B^2)\tan\alpha+m/N-(m/N)r_m(nb\sec\pi/N)].$$

Experimental validitation

The atomized iron powder of greater than 99% purity and finer than 150 micron was procured from LOBA CHEMICALS, Bombay. Table 1 gives the physical and chemical analyses of this atomized powder.

The iron powder was compacted in a closed cylindrical die using a 150 ton press. The die wall was lubricated with graphite powder. Six compacts were prepared by using square, pentagonal, and hexagonal die and punch sets under same conditions and these were sintered at about 1,100 °C in Argon atmosphere for about 2 h. The average relative density of the sintered preforms was found to be around 0.82. Then the center of each of these specimens was given shapes of square, pentagonal, and hexagonal by machining processes. Samples of each type were made with different thickness and height to get varying aspect ratios. The surfaces of the specimens were then polished with fine emery paper. These specimens were then placed between the dies of a 100-ton Hydraulic press and were cold pressed until cracks formed at the peripheral surface. The barreling effect was clearly visible in each cases. The applied loads against the percentage reduction of the sample heights were recorded and a curve was drawn for the experimental condition (Tables 2–7). This was then compared with the theoretical plots of applied load versus percentage deformation calculated for different values of the barreling parameter 'β'. They give us an idea about the extent of barreling under the experimental condition. Both the theoretical and experimental calculations assumed an initial relative density of the sintered preform to be 0.82.

Conclusion

The sintered components are very sensitive to hydrostatic stresses and relative density changes during the deformation process, consequently the mode of plastic deformation of sintered components are different from wrought metals.

Table 2 Experimental and theoretical readings for square sample no.1

Percentage deformation	Load applied (kgf)						
	Experimental values (B)	Theoretical values					
		(C) $\beta = 0.15$	(D) $\beta = 0.25$	(E) $\beta = 0.35$	(F) $\beta = 0.45$	(G) $\beta = 0.55$	(H) $\beta = 0.65$
10	3,200	1,820	2,100	3,720	3,920	4,100	4,350
20	6,400	3,040	3,560	6,840	7,200	7,420	7,780
30	15,640	7,420	8,480	14,520	14,880	15,240	15,870

Table 3 Experimental and theoretical readings for square sample no.2

Percentage deformation	Load applied (kgf)						
	Experimental values (B)	Theoretical values					
		(C) $\beta = 0.15$	(D) $\beta = 0.25$	(E) $\beta = 0.35$	(F) $\beta = 0.45$	(G) $\beta = 0.55$	(H) $\beta = 0.65$
10	3,000	1,640	1,920	2,460	3,200	3,600	4,220
20	7,200	3,320	3,640	5,880	6,460	7,560	7,840
30	14,800	7,760	8,440	110,780	13,280	14,520	14,960
35	16,000	11,440	12,240	13,320	14,460	15,660	16,240

Table 4 Experimental and theoretical readings for pentagonal sample no.1

Percentage deformation	Load applied (kgf)						
	Experimental values (B)	Theoretical values					
		(C) $\beta = 0.15$	(D) $\beta = 0.25$	(E) $\beta = 0.35$	(F) $\beta = 0.45$	(G) $\beta = 0.55$	(H) $\beta = 0.65$
10	8,200	6,400	7,560	8,020	8,620	8,900	9,220
15	14,400	11,560	13,580	14,200	14,820	15,120	15,880
20	17,600	15,420	16,220	17,060	17,880	18,020	18,400

Table 5 Experimental and theoretical readings for pentagonal sample no.2

Percentage deformation	Load applied (kgf)						
	Experimental values (B)	Theoretical values					
		(C) $\beta = 0.15$	(D) $\beta = 0.25$	(E) $\beta = 0.35$	(F) $\beta = 0.45$	(G) $\beta = 0.55$	(H) $\beta = 0.65$
10	6,200	5,860	6,060	6,960	7,220	7,980	8,600
15	15,800	11,020	13,440	14,820	15,660	16,240	16,860
20	17,100	14,960	15,820	16,900	17,400	17,980	18,020

Table 6 Experimental and theoretical readings for hexagonal sample no.1

Percentage deformation	Load applied (kgf)						
	Experimental values (B)	Theoretical values					
		(C) $\beta = 0.15$	(D) $\beta = 0.25$	(E) $\beta = 0.35$	(F) $\beta = 0.45$	(G) $\beta = 0.55$	(H) $\beta = 0.65$
10	7,400	5,280	6,660	7,620	8,040	8,480	8,900
15	15,600	13,020	14,880	15,890	16,400	16,920	17,320
20	18,400	16,680	17,520	18,340	18,820	19,120	19,480

Table 7 Experimental and theoretical readings for hexagonal sample no.2

Percentage deformation	Load applied (kgf)						
	Experimental values (B)	Theoretical values					
		(C) $\beta = 0.15$	(D) $\beta = 0.25$	(E) $\beta = 0.35$	(F) $\beta = 0.45$	(G) $\beta = 0.55$	(H) $\beta = 0.65$
10	7,800	5,100	6,480	7,780	8,320	8,630	8,800
15	16,400	12,720	14,620	15,420	16,760	17,260	17,630
20	19,200	16,040	17,020	17,840	18,980	19,540	19,900

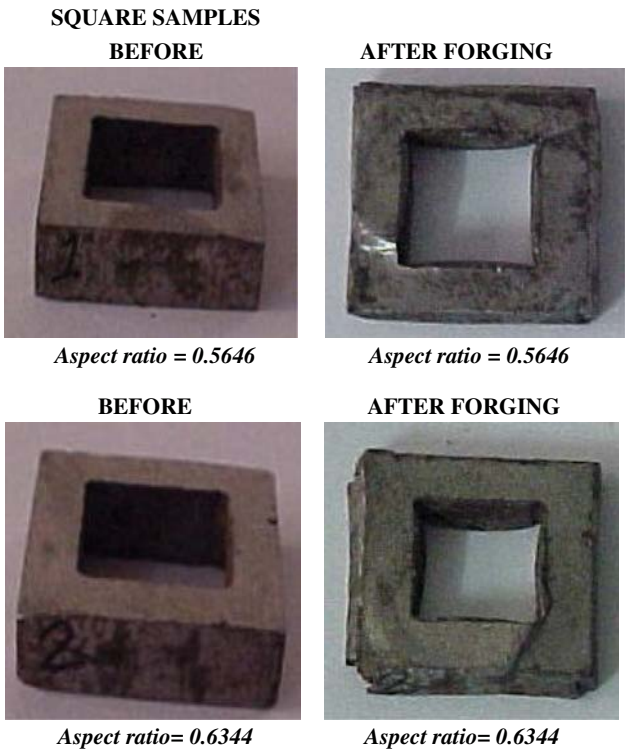

Fig. 2 Square samples of aspect ratio 0.5646 and 0.6344 before and after forging

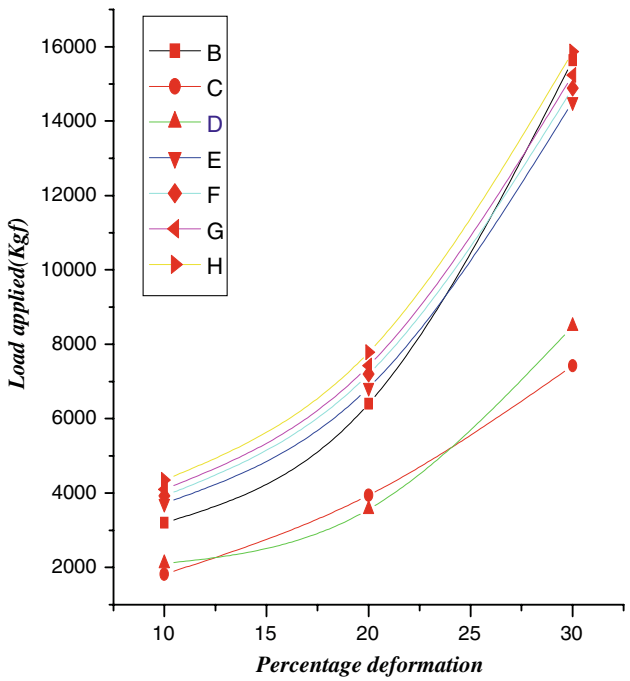

Graph 1 Forging load versus percentage reduction of square samples of aspect ratio 0.5646

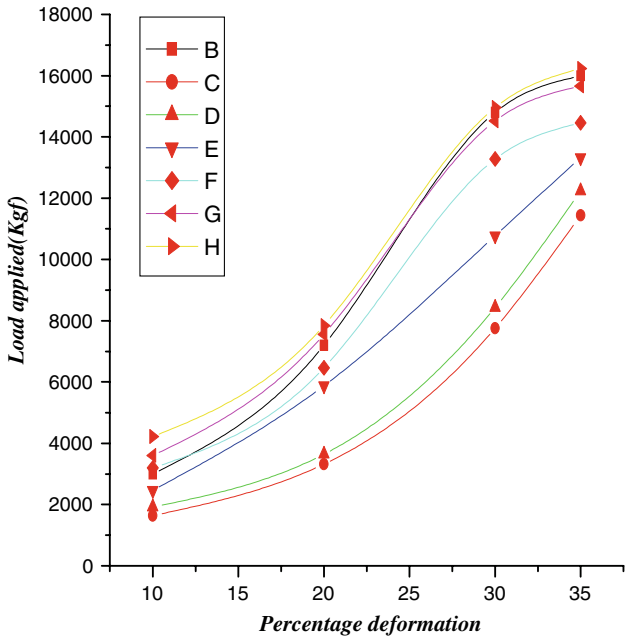

Graph 2 Forging load versus percentage reduction of square samples of aspect ratio 0.6344

Fig. 3 Pentagonal samples of aspect ratio 0.4678 and 0.621 before and after forging

During compression of metal-powder preforms by flat dies under axi-symmetric condition it has been seen that consolidation and compression both take place simultaneously. At the beginning of the compression process the pores of the preform gets elongated in the direction of spreading and compressed in the perpendicular direction of spreading and finally closes. As a result the relative density of the sintered samples changes

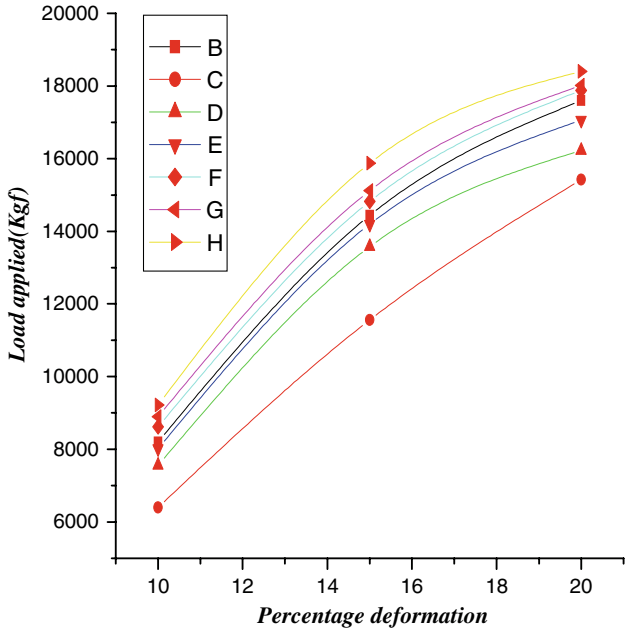

Graph 3 Forging load versus percentage reduction of pentagonal samples of aspect ratio 0.4678

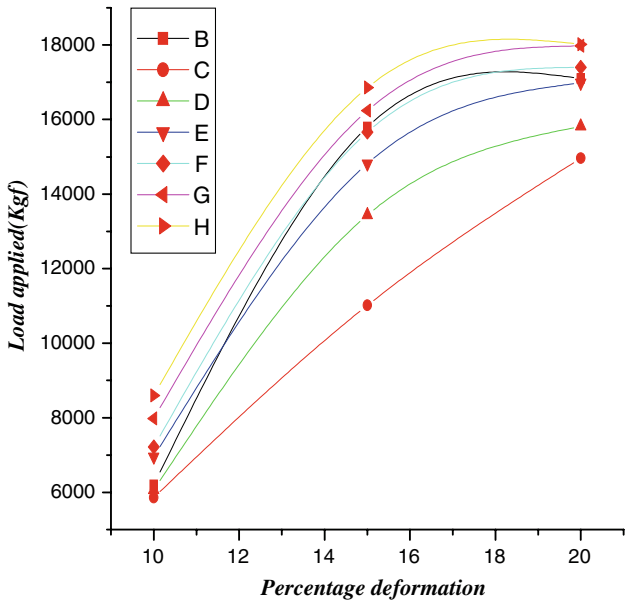

Graph 4 Forging load versus percentage reduction of pentagonal samples of aspect ratio 0.621

sharply during the beginning stage of pressing and then changes linearly with the increase in load.

In this present investigation, a general equation for the forging of 'square' hollow polygonal disk has been derived under dry condition and then different aspect ratios were considered as particular cases to be investigated under it (Fig. 2, Graphs 1, 2). The results derived from the analysis are being verified along with experimental results. The mode of forging is considered as axi-symmetric (identical flow

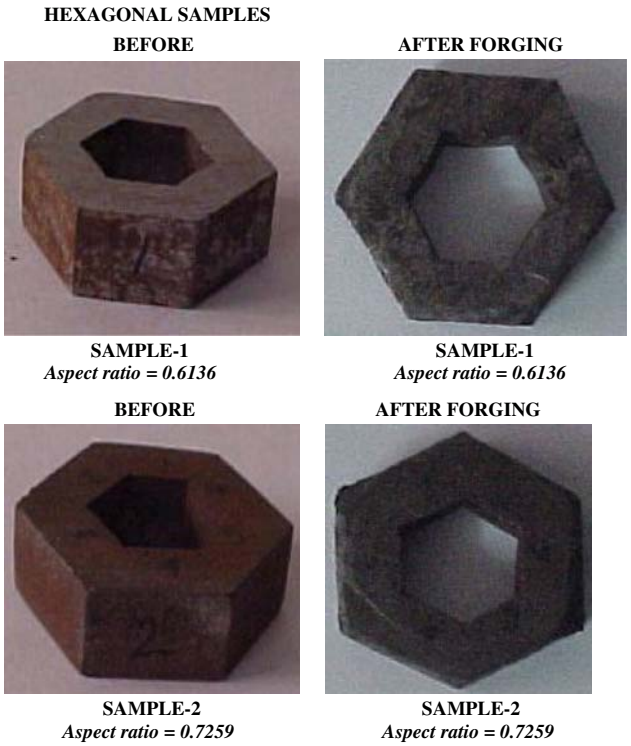

Fig. 4 Hexagonal samples of aspect ratio 0.6136 and 0.7259 before and after forging

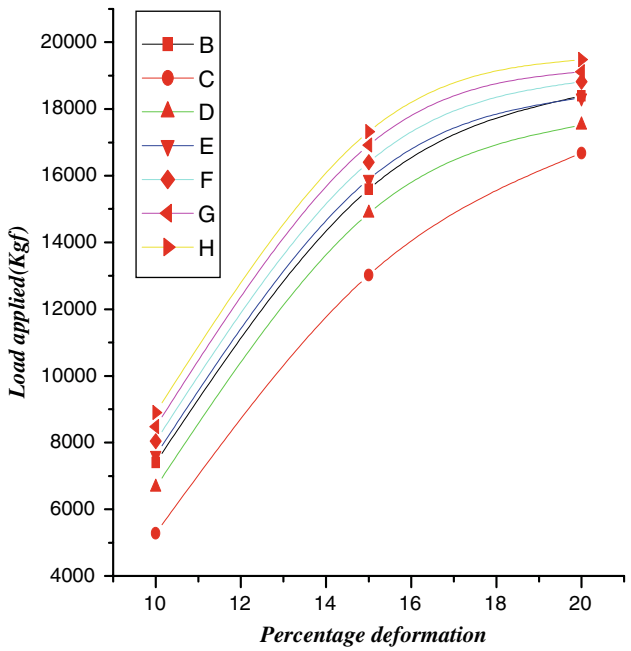

Graph 5 Forging load versus percentage reduction of hexagonal samples of aspect ratio 0.6136

considerations) and bulging parameter 'β' has been considered under a couple of aspect ratios for each sample. It have been observed that 'β' value increases with increase in aspect ratio for all polygonal disks (Fig. 3, Graphs 3, 4; Fig. 4,

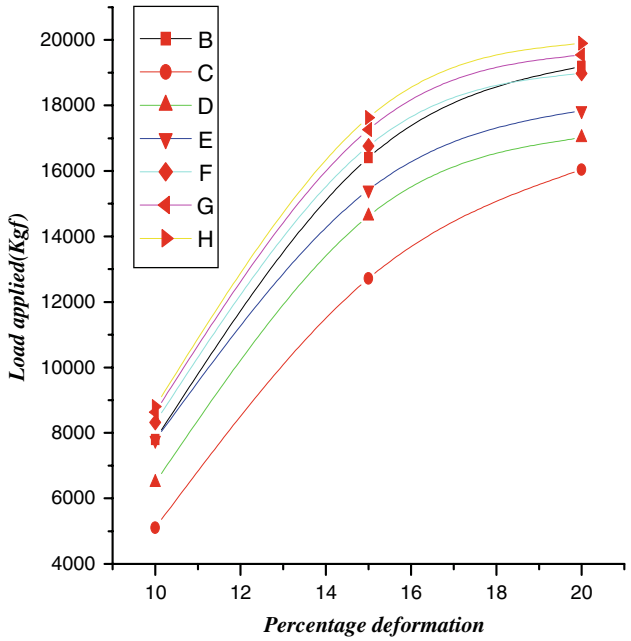

Graph 6 Forging load versus percentage reduction of hexagonal samples of aspect ratio 0.7259

Graphs 5, 6). Though an extensive study is required to arrive at a final conclusion regarding the matter. The effects of tribological conditions are of immense importance during the deformation of polygonal disks.

Hopefully, this present work throws a light on the immense potential regarding the forging of sintered hollow polygonal disks under dry condition. The feasibility of processing of different hollow polygonal disks has been demonstrated in this thesis, which is supposed to be helpful in predicting the formability or forgeability of the components. The forgeability or the formability is also estimated for above-mentioned deforming conditions which will be of immense importance in designing the equipment and tooling required for cold forging of metal-powder preforms. It is expected that these investigations will be helpful in understanding the deformation pattern and fracture behavior during open die forging of metal-powder preforms.

References

1. Juneja BL (1973) Int J Mach Tool Des Res 13:87
2. Sutradhar G, Jha AK, Kumar S (2000) J Inst Eng (India) 81:130
3. Tabata T, Masaki S (1980) Int J Powder Metall Powder Technol 16:149
4. Wittenaur J (1997) Mater Sci Forum 273:243
5. Ranjan S, Kumar S (2004) Tamkang J Sci Eng 7(1):53
6. Agarwal M, Kumar S, Jha AK (1999) J Inst Eng (India)-PR 80:8
7. Ranjan S, Kumar S (2004) J Sci Engb 7(4):219
8. Sutradhar G, Kumar S, Agarwal M (2002) J Mater Process Technol 123:440